Las Pailas 35 MW (Net) Binary Power Plant, Rincón de la Vieja, Guanacaste, Costa Rica

Paul Moya[1] and Ronald DiPippo[2]

[1]Geothermal Energy Consultant, Guanacaste, Costa Rica
[2]Renewable Energy Consultant, South Dartmouth MA, USA

Keywords

Las Pailas, Costa Rica, well data, binary power plant, cycle analysis, thermal efficiency, utilization efficiency, availability, plant factor, environmental impact

ABSTRACT

The Las Pailas geothermal power station, the second field in Costa Rica to achieve commercial operation, is described. The drilling of the wells and well-field layout and constraints are presented. The design of the unique 2-unit binary power plant is discussed in detail. Plant performance is assessed based on the design specifications and on actual operations, from both a cycle and an overall plant perspective. Thermal and utilization efficiencies are calculated. The normal-pentane power cycle is shown to scale in pressure–enthalpy and temperature–entropy diagrams. The analysis of data for the first eight months of plant operation indicates that the average plant (or capacity) factor was 90.1% and the plant was available and generating power 91.7% of the time. So far there are no discernible environmental impacts from plant operations.

Introduction

Costa Rica is located toward the southern end of Central America, between Nicaragua on the northwest and Panama on the southeast. The country covers an area of approximately 51,100 km^2 and has a population of 4.64 million [1]. As of 2008, Costa Rica had an installed electric power capacity of 2,378 MW of which geothermal power plants contributed 163 MW, or about 6.9%. The country consumed about 8,250 GWh of electricity of which about 1,070 GWh, or about 13.0%, came from geothermal units [1, 2]. Although the country has several geothermal areas with potential that stretch along the central cordillera, the most important ones are located in the northwest part in the Guanacaste province on the southwestern slopes of the Miravalles and the Rincón de la Vieja volcanoes; see Figure 1.

History of Exploration at the Rincón de la Vieja Volcanic Area

Geothermal studies at the Rincón de la Vieja volcanic area (RDLV) began in 1963 under the auspices of the United Nations (U.N.). The Costa Rican Electricity Institute (ICE), or Instituto Costarricense de Electricidad, in Spanish, requested the U.N. to send a team of geothermal experts to survey the RDLV and nearby areas [4]. The first phase of a detailed reconnaissance of the area was carried out more than ten years later by ICE with assistance from Rogers Engineering and GeothermEx in 1975-76. The best three prospective sites were identified as the Miravalles, RDLV, and Tenorio volcanic zones [5]. Following the publication of the report in 1976, the Miravalles volcanic area was selected for development and the RDLV was set aside for more than a decade. Some additional studies were carried out there in 1987 and 1988 by ICE with assistance from the Ente Nazionale per l'Energia Elettrica of

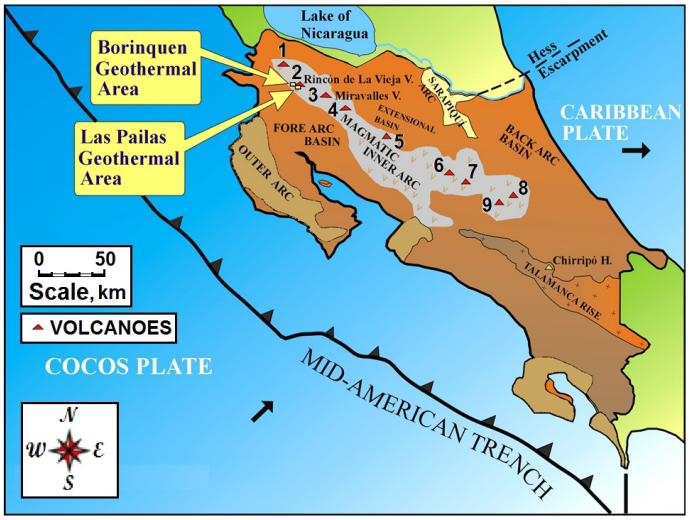

Figure 1. Costa Rica's geothermal fields and prospects, after [3]. Volcanoes: 1-Orosi, 2-Rincón de la Vieja, 3-Miravalles, 4-Tenorio, 5-Arenal, 6-Poas, 7-Barba, 8-Turrialba, 9-Irazu.

Italy (ENEL) [6]. Various scientific studies were conducted over the years, culminating with the drilling of nine thermal gradient wells in starting in May 1994 and continuing to 1996 [7].

Once the Miravalles field was built out to its maximum sustainable capacity, ICE turned its attention back to the RDLV area. Three zones marked by surface thermal manifestations were explored: Las Pailas, Las Hornillas, and Borinquen, all lying on a NW-SE line roughly parallel to and south of the main axis of the RDLV complex; see Figure 2.

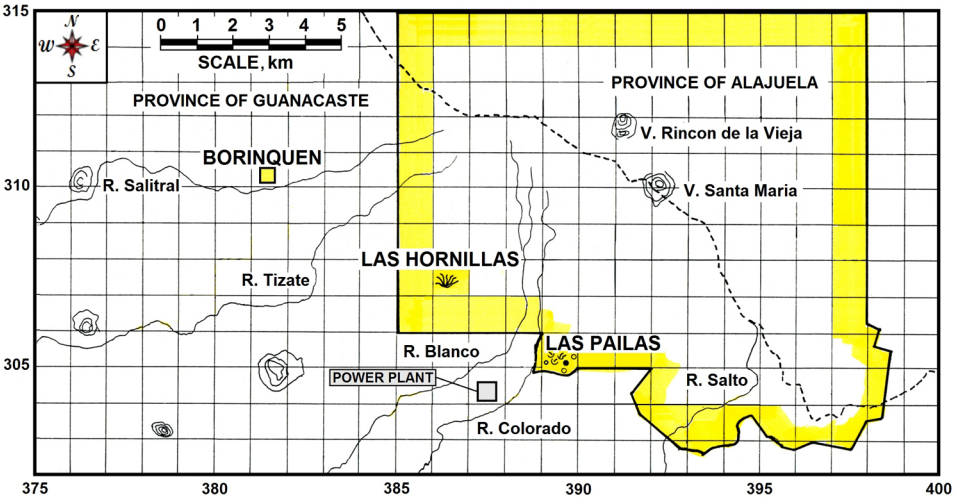

Figure 2. Borinquen, Las Hornillas and Las Pailas geothermal areas at the Rincon de la Vieja volcanic area. National Park boundary is highlighted.

Las Pailas is host to the most extensive and spectacular geothermal manifestations in Costa Rica, including steaming ground, fumaroles, steam-heated boiling springs, and mud pots and pools. The area of concentrated manifestations lies just inside the boundary of the RDLV National Park. Las Hornillas is a very small fumarolic area upslope on the flank of RDLV volcanic complex, whereas Borinquen displays significant boiling mud pots. So far ICE has drilled two wells at Borinquen which are hot and deep: PGB-01 at 278^{0}C and 2,594 m, and PGB-03 at 203^{0}C and 2,082 m; however, both wells exhibit very low permeability. Currently ICE is preparing the access roads and well pads to drill additional deep wells to develop the Borinquen area as the next geothermal field in Costa Rica. The entire Borinquen area is renowned for its ecotourism; two upscale hotel-resorts are close to the field.

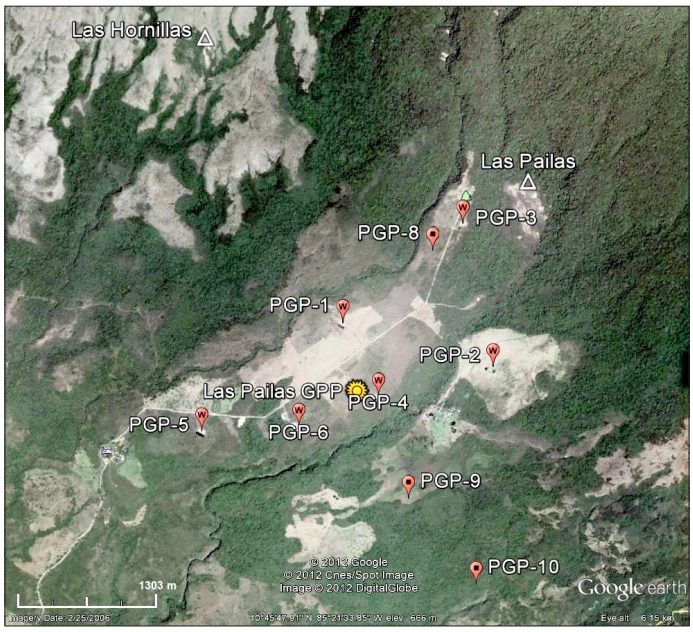

Figure 3. Well pad locations at Las Pailas (PGP-9 and PGP-10 approx). *Google Earth*, image date 2/25/2006, accessed 3/5/2012.

Las Pailas Well Drilling Program and Results

The Las Pailas geothermal field lies on a generally smooth plain, probably an ancient avalanche, which gradually slopes up to the northeast along the southwestern flank of the RDLV volcanic area. The pre-feasibility study at Las Pailas was commissioned by ICE and carried out by GeothermEx, Inc. from April 1999 with the final report being delivered in December 2001 [8]. Five drill sites were recommended in the Las Pailas area. Four wells were programmed for each site to confirm the presence of a geothermal reservoir and to develop sufficient geofluid to support a commercial power plant. A fifth well site was designated as a development well at the periphery of the field where residual geothermal fluid could be re-injected.

Table 1. Some characteristics of Las Pailas wells as of March 2012.

Well No.	Depth (m)	Temp. (°C)	Enthalpy (kJ/kg)	Power (MW)
PGP-01	1,418	254	1,106	9.1
PGP-02	1,764	240	NA	NA
PGP-03	1,772	252	1,335	4.5
PGP-04	1,418	232	1,011	NA
PGP-05	1,827	160	NA	NA
PGP-06	1,327	200	NA	NA
PGP-08	1,712	240	1,072	4.9
PGP-09	1,742	203	NA	NA
PGP-10	2,673	230	NA	NA
*PGP-11	1,703	238	1,024	9.6
*PGP-12	1,694	256	1,116	8.3
**PGP-16	510	NA	NA	NA
*PGP-17	1,523	244	1,057	11.8
*PGP-19	924	235	NA	NA
*PGP-20	690	230	NA	NA
*PGP-23	2,169	233	NA	NA
*PGP-24	1,544	184	1,086	NA
*PGP-25	1,478	245	1,000	NA
*PGP-27	1,814	160	NA	NA

*-Deviated well **-Deviated well in progress NA-Not available

Given the proximity to the RDLV National Park and the NGO Guanacaste Dry Forest, the well sites were severely restricted. In fact ICE is constrained to develop a relatively small parcel of land, roughly 4 km by 3 km [9].

Figure 3 shows the first nine wells drilled. The most productive area so far lies between the Rio Blanco and Rio Colorado, which in this area are roughly parallel and trending northeast, the same direction as several identified faults.

The terrain in the well field rises gradually from an elevation of about 557 masl at PGP-05 to 764 masl at PGP-03 over a distance of roughly 3 km. The northernmost well pad lies 700 m west of the area of strongest thermal manifestations. As of March 2012, 18 wells have been completed, half vertical and half directional; one well, PGP-16 is in progress; see Table 1.

The casing profiles for the six current producing wells are shown in Figure 4. Surface casings are all 18-5/8", followed by 13-3/8" casings. Wells PGP-01, 08 and -12 have 10-3/4" slotted liners in the production zone; wells PGP-03 and -11 have 9-5/8" casings followed by 7-5/8" slotted liners; and well PGP-17 has a 9-5/8" casing followed by a 9-5/8" slotted liner or 9-5/8" followed by another 9-5/8" casing and finishes with a 7-5/8" slotted liner.

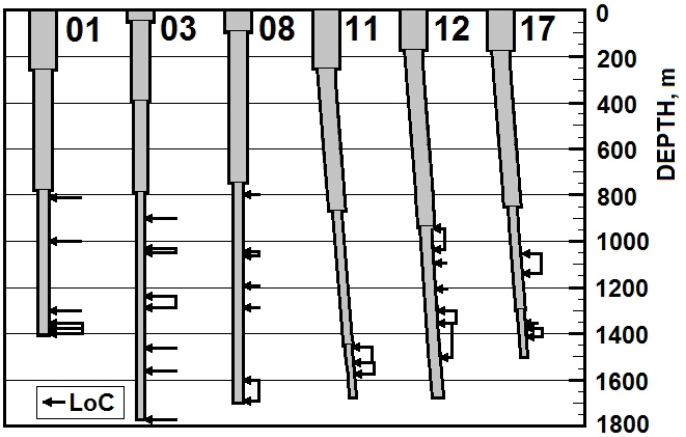

Figure 4. Casing profiles and feed zones for six producing wells. LoC = loss of circulation; horizontal deviations are not to scale.

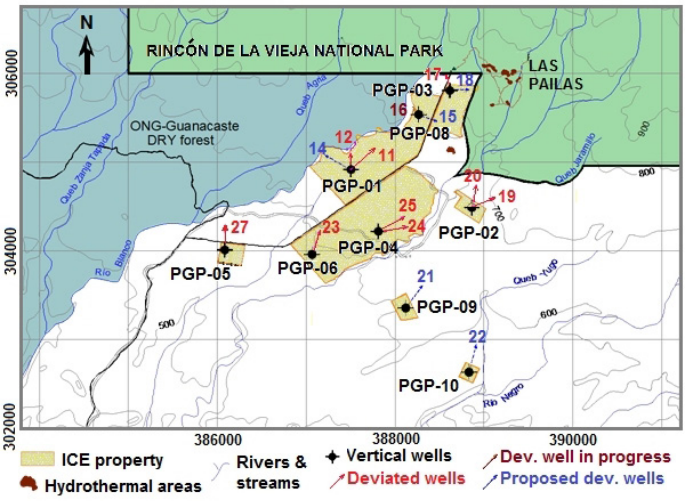

Figure 5. Wells drilled at Las Pailas as of March 2012, after [9].

The well map showing all the wells and their directions is given in Figure 5. The gathering system is shown in a line drawing in Figure 6 and in schematic form in Figure 7.

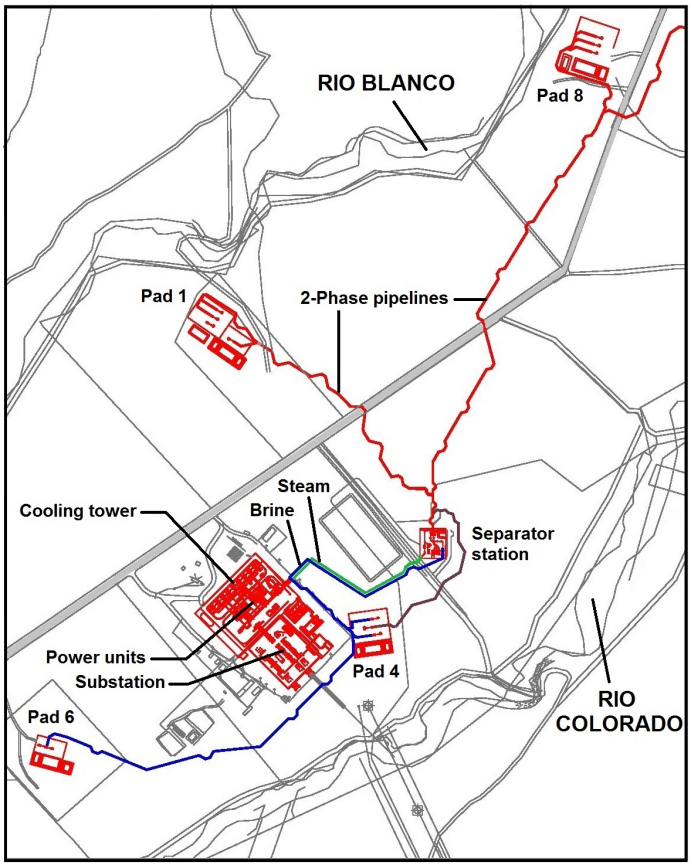

Figure 6. Gathering system. Note Pad 3 is beyond the diagram at upper right.

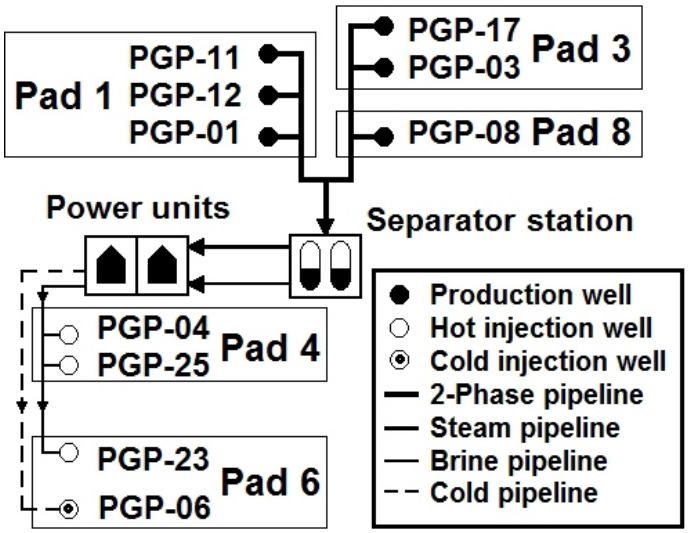

Figure 7. Simplified line diagram of the geofluid gathering system.

Wells PGP-17, -11 and -01 are the most prolific wells, as can be seen for the production curves displayed in Figures 8 and 9.

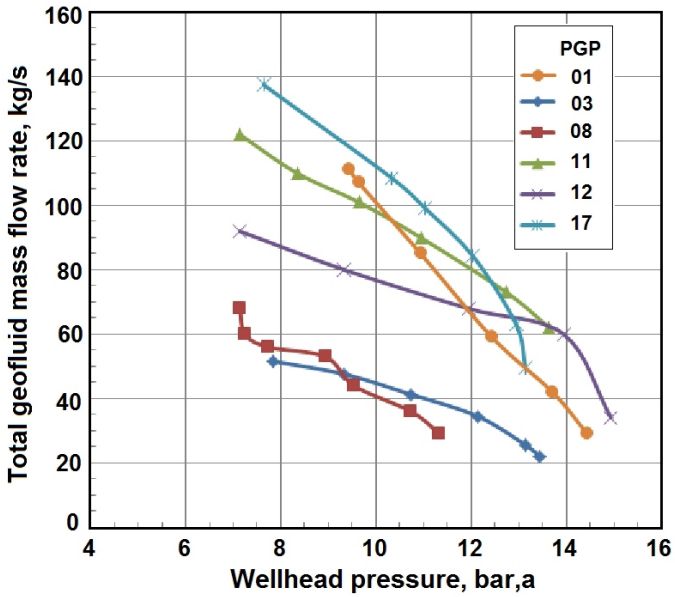

Figure 8. Production curves for six wells.

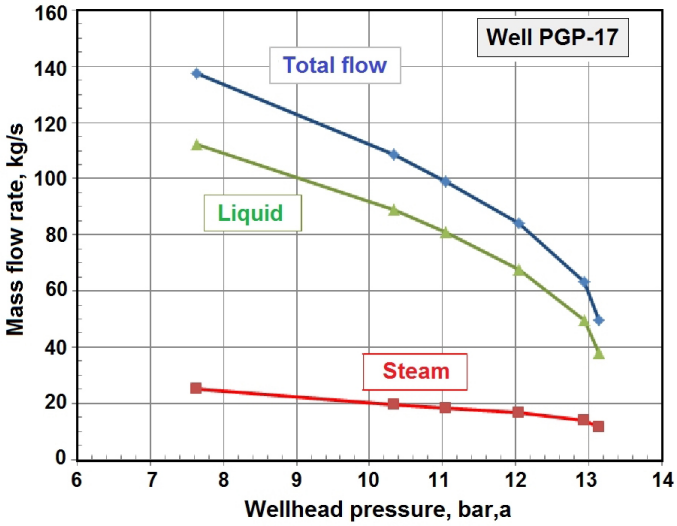

Figure 9. Production flow information for well PGP-17.

There are three "hot" reinjection wells to handle the brine leaving the heat exchangers of the power units, namely, PGP-04, -23 and -25; the brine return temperature is about 140°C. One well PGP-06 is dedicated to the injection of "cold" brine which includes cooling tower blowdown and any brine that has collected in the holding pond in the course of operations; this temperature varies widely from about 30 to 80°C.

Power Plant Design

The 41.6 MW (gross) Las Pailas binary geothermal power plant was inaugurated on July 24, 2011 by Costa Rica´s President Laura Chinchilla. The choice of a binary-type power cycle for a high-temperature, liquid-dominated field producing a 2-phase mixture of liquid and vapor is somewhat unconventional. Typically a flash design would be selected, as was the case for the three main units at the nearby Miravalles station [10]. However, only one company bid on the project [3] and that company specializes in binary plants.

Given the proximity of the site to the Rincón de la Vieja National Park and the high frequency of tourists passing close by the plant site every day, ICE carefully selected the plant site so as to minimize the visual impact on the surroundings. As can be seen from Figure 10, the plant has a low profile with no steam venting in sight.

Figure 10. Overview of plant, looking generally west; holding pond for cold reinjection in foreground; the main road is off to the right, roughly parallel to the cooling tower. Photo by P. Moya.

All the geofluid is collected from the six producing wells by means of large diameter 2-phase flow pipelines and delivered to the separator station where two vertical cyclone separators create streams of steam and liquid (brine); see Figure 11. The two streams are conveyed to the heat exchangers of the organic Rankine cycle (ORC). The preheaters and evaporators are shell-and-tube type with the steam and brine inside the tubes; the condensers are also shell-and-tube with cooling water inside the tubes. Recuperators are likewise shell-and-tube with the high-pressure N-pentane inside the tubes and the low-pressure N-pentane on the shell side. In all cases the tube bundles are fixed in place. In general, all equipment is similar to what is installed at Miravalles Unit 5, but larger to accommodate the higher power output [11].

Figure 11. Separator station; twin cyclone separators in foreground and bank of silencers in background. Photo by P. Moya.

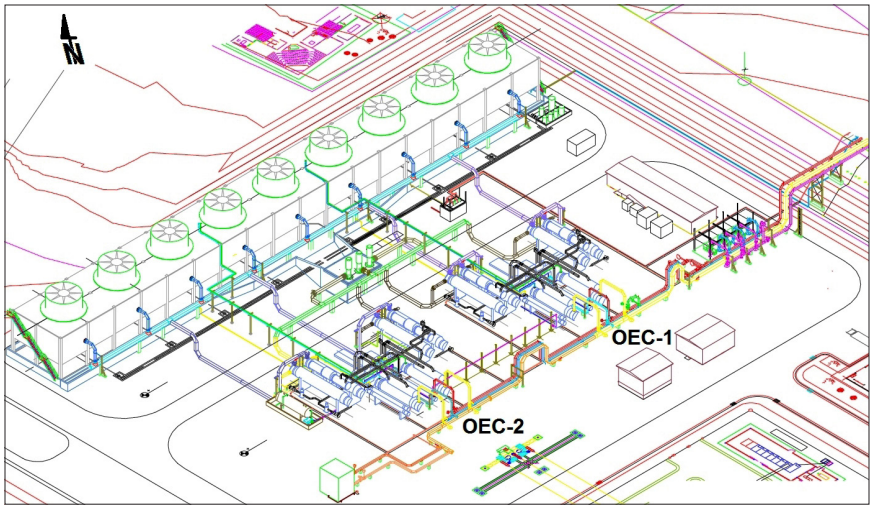

Figure 12. Isometric rendering of plant, after [3].

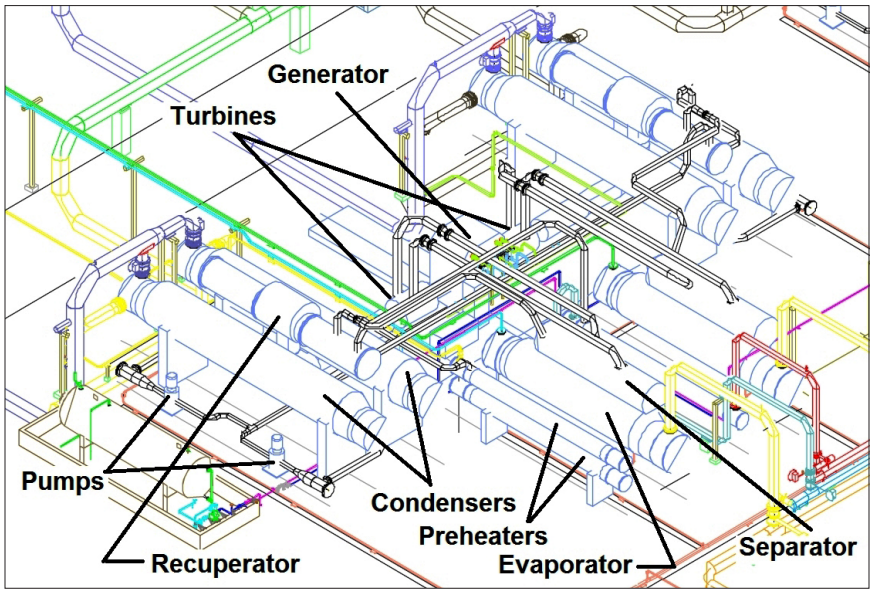

Figure 13. Detailed isometric of one OEC unit; there are 2 evaporators, 2 separators, 2 turbines, 4 condensers, 2 recuperators, 4 pumps and 1 generator per OEC unit. Turbines and generator are housed within a building, after [3].

The isometric sketch in Figure 12 depicts overall layout of the plant, including the two power units, heat exchangers, 9-cell cooling tower, and steam and brine pipelines. Figure 13 shows one of the two ORC units in an isometric line drawing [3]. Figure 14 is a photograph of the two ORCs taken from the southwest end of the cooling tower.

To aid in the analysis of the plant, a simplified flow diagram is helpful; see Figure 15. Next a plant flow diagram, Figure 16 (next page), was prepared showing all the major components and important thermodynamic state points. Since there is only one electrical generator per unit, driven by two separate turbines, for analysis the unit may be divided into two halves that we have arbitrarily called the Left and Right sides in Figure 16. This is important because the two sides are not symmetrical with respect to thermodynamic function, as we will see in the next section.

Plant Performance – Design Case

The performance of the Las Pailas plant will be analyzed using the design specifications from the manufacturer of the energy conversion equipment, Ormat, Inc. Using the heat balance diagram for 100% load, the cycle processes will be shown in temperature-entropy (T-s) and pressure-enthalpy (P-h) diagrams, and various energy terms will be calculated with the aid of REFPROP software [12]. Cycle and plant efficiencies will be computed using the First and Second Laws of thermodynamics.

Each OEC power unit consists of two interlocked Rankine cycles, arbitrarily designated here as the "Left-side" and the "Right-side" for ease of reference. The Left-side cycle is shown in Figure 17, a temperature-entropy (T-s) diagram. The numbered

Figure 14. Power houses for Unit 1 (left) and Unit 2 (center). Condensers and recuperators are the dark-colored horizontal vessels adjacent to the buildings; the N-pentane holding tank is the yellow horizontal vessel at the right. Photo by P. Moya.

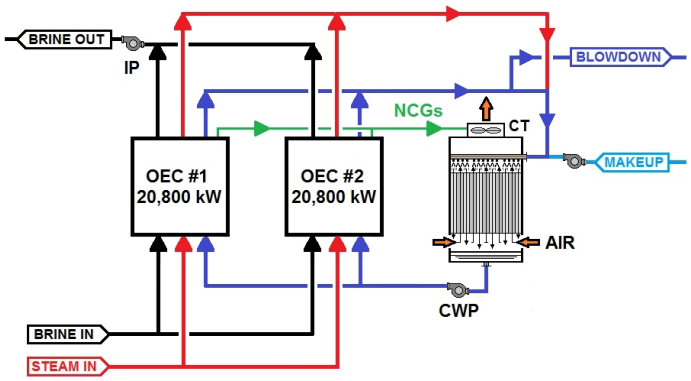

Figure 15. Overall plant schematic flow diagram.

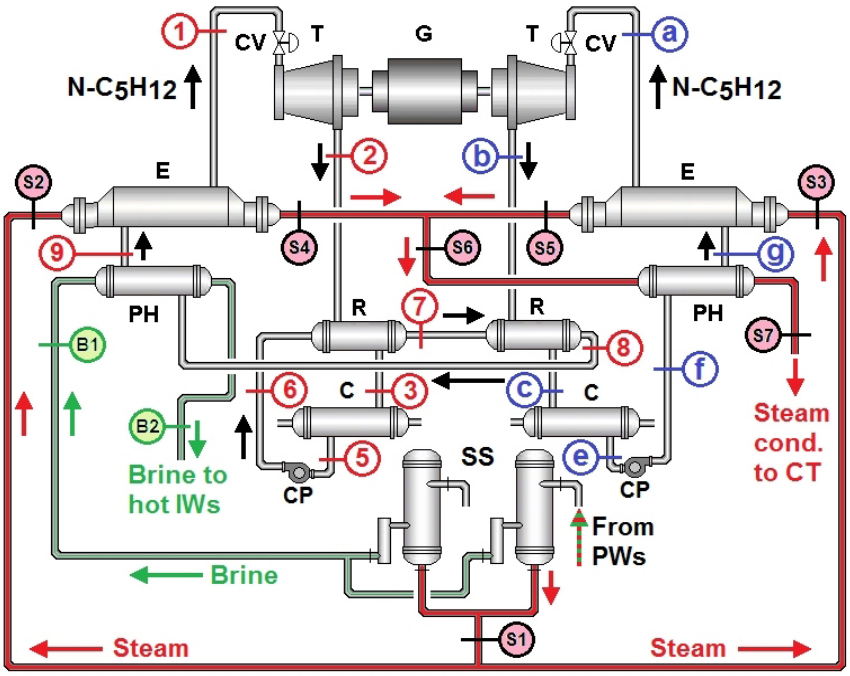

Figure 16. Simplified plant schematic flow diagram; red state-point numbers refer to the arbitrarily denoted "Left-Side" of the cycle and blue lower-case letters refer to the "Right-Side"; black S-numbers refer to steam & condensate and green B-numbers refer to brine. Note the cycle is asymmetric with regard to flows through the recuperators.

state-points represent the design values taken for the design heat balance diagram. The processes are as follows:

1-2: turbine expansion (power generation)
1-2s: ideal turbine expansion (isentropic)
2-3: heat delivered to Left recuperator
3-4: desuperheat in condenser
4-5: heat discharged in condenser
5-6: pressurization of liquid in feed pump
5-6s: ideal isentropic pressurization (not shown)
6-7: heat received in Left recuperator
7-8: heat received in Right recuperator
8-9: heat received in Left preheater
9-1: heat received in Left evaporator.

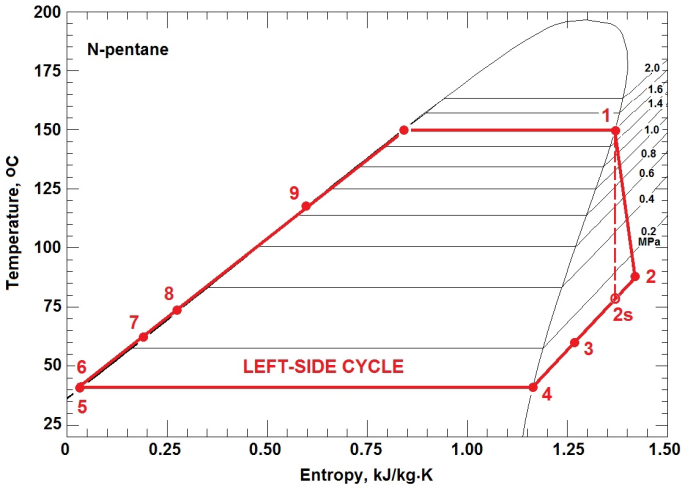

Figure 17. Temperature-entropy process diagram for the Left-Side of one of the two OECs; design case.

Although the equipment layout is symmetrical about a centerline through the single generator, the working fluid flow paths for the Left- and Right-side cycles are not. The N-pentane leaving the Left turbine passes through the Left recuperator before entering the Left condenser, and the N-pentane leaving the Right turbine passes through the Right recuperator before entering the Right condenser. However, the N-pentane return from the Left feed pump passes through the Left recuperator and the Right recuperator, in sequence, before entering the Left preheater, whereas the N-pentane return from the Right feed pump passes directly to the Right preheater. Thus, both turbines contribute heat to the recuperators but only the Left cycle benefits from that heat.

Figure 18 shows the same processes from Figure 17 but in a pressure-enthalpy (P-h) diagram; note the logarithmic scale on the pressure axis. Note also that the pressure loss between the feed pump outlet and the turbine inlet has been arbitrarily assigned to the heat exchanger train consisting of the two recuperators and the preheater. It was assumed that there was a 5% drop in pressure through each heat exchanger; this allowed the pump outlet pressure to be calculated from the known turbine inlet pressure.

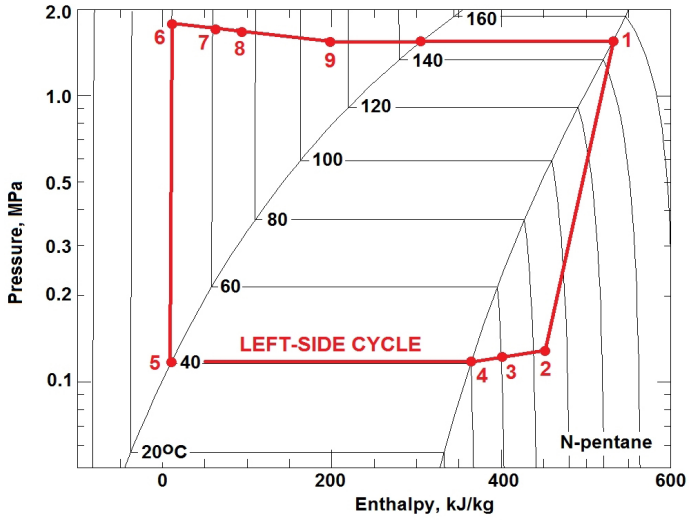

Figure 18. Pressure-enthalpy process diagram for the Left-Side of one of the two OECs.

Figure 19 shows the P-h diagram for the processes in the Right-side of the OEC. The processes are as follows:

a-b: turbine expansion (power generation)
a-bs: ideal isentropic turbine expansion (not shown)
b-c: heat delivered to Right recuperator
c-d: desuperheat in condenser
d-e: heat discharged in condenser
e-f: pressurization of liquid in feed pump
e-fs: ideal isentropic pressurization (not shown)
f-g: heat received in Right preheater
g-h: sensible heat received in Right evaporator
h-a: latent heat received in Right evaporator.

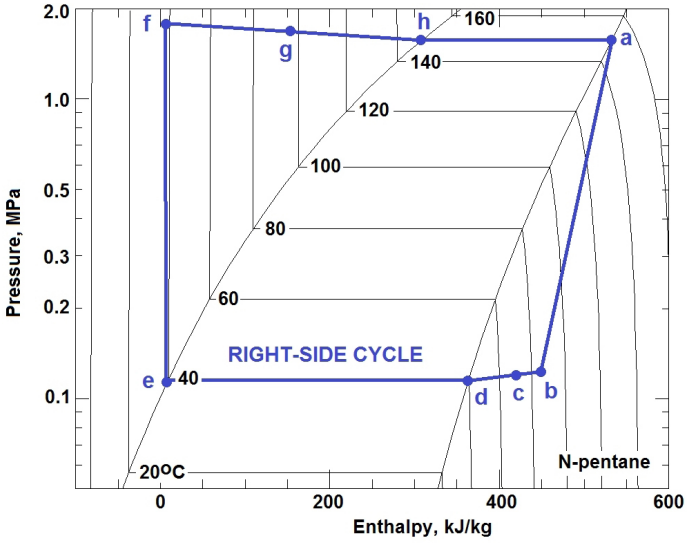

Figure 19. Pressure-enthalpy process diagram (to scale) for the Right-Side of one of the two OECs.

Tables 2, 3, and 4 present the design state-point properties for the N-pentane working fluid, the geothermal steam and brine. Most of these values were taken directly from the Ormat design heat balance diagram (HBD), but some were obtained by making certain assumptions. For example the inlet state for the Left turbine as defined on the HBD by the temperature of 148.1°C and a pressure of 1.549 MPa (Table 2) is actually a subcooled liquid according the REFPROP; this is unrealistic. Either the stated temperature is too low (i.e., below the saturation temperature for the stated pressure) or the pressure is too high (i.e., above the saturation pressure for the stated temperature). Since we cannot be sure which is true, or whether the problem lies in the particular set of property values used, the assumption was made for the purpose of calculation that the turbine inlet is a saturated vapor at the stated temperature; the enthalpy and entropy values thus correspond the saturated vapor at a temperature of 148.1°C, the corresponding saturation pressure would be 1.539 MPa.

Although the generator output for each OEC is given as 20,800 kW, the individual power output of the two turbines is not given on the HBD. The assumption was made that the specific power output, in kJ/kg or kW/(kg/s), is the same for the two turbines. Thus, knowing the respective mass flow rates allows the calculation of the individual turbine power outputs.

Using standard working equations for the heat and work terms in the cycle [13], all energy terms may be calculated; the results are shown in Table 5.

Table 2. Design state-point properties: Left-side of cycle; N-pentane mass flow = 145.1 kg/s.

State	Temperature °C	Pressure MPa	Enthalpy kJ/kg	Entropy kJ/kg.K
1	148.1	1.5490	531.34	1.3655
2s	79.5	0.1325	436.56	1.3655
2	88.4	0.1325	453.90	1.4140
3	60.4	0.1262	400.46	1.2656
4	41.2	0.1202	365.58	1.1633
5	38.4	0.1202	5.560	0.0178
6s	39.0	1.7932	8.310	0.0178
6	39.7	1.7932	9.967	0.0231
7	61.2	1.7078	62.17	0.1849
8	71.5	1.6265	88.04	0.2615
9	117.0	1.5490	210.62	0.5955

Table 3. Design state-point properties: Right-side of cycle; N-pentane mass flow = 123.5 kg/s.

State	Temperature °C	Pressure MPa	Enthalpy kJ/kg	Entropy kJ/kg.K
a	150.1	1.6030	533.97	1.3689
bs	79.0	0.1263	435.91	1.3689
b	89.6	0.1263	456.54	1.4266
c	72.1	0.1203	422.80	1.3367
d	39.7	0.1146	363.31	1.1613
e	37.0	0.1146	2.230	0.0071
fs	37.6	1.7673	4.940	0.0071
f	38.3	1.7673	6.624	0.0125
g	97.0	1.6832	154.98	0.4485
h	150.1	1.6030	312.47	0.8455

Table 4. Design state-point properties for steam and brine.

State	Temperature °C	Pressure MPa	Enthalpy kJ/kg	Entropy kJ/kg.K	Mass Flow kg/s
Steam & condensate state-points					
S1	158.4	0.6	2755.67	6.7629	44.5
S2	158.4	0.6	2755.67	6.7629	22.25
S3	158.4	0.6	2755.67	6.7629	22.25
S4	145.56	0.57	613.14	1.7963	21.8
S5	145.56	0.57	613.14	1.7963	21.8
S6	145.56	0.57	613.14	1.7963	43.6
S7	45.4	0.5415	190.57	0.6436	43.6
Brine state-points					
B1	162	0.74	684.22	1.9624	188.89
B2	140	0.54	589.28	1.7390	188.89

Table 5. Calculated cycle results for design case: one OEC.

Item	Left-Side Cycle	Right-Side Cycle
Specific turbine power, kJ/kg	77.438	77.439
Gross turbine power, kW	11,236	9,564
Turbine isentropic efficiency	0.817	0.790
Specific pump power, kJ/kg	4.408	4.395
Pump power, kW	639.6	542.7
Pump isentropic efficiency	0.624	0.617
Evaporator heat duty. kWt	46,537	46,806
Condenser heat duty, kWt	57,300	51,940
Preheater heat duty, kWt	17,786	18,321
Heat delivered to Left recuperator, kWt	7,753.8	
Heat acquired in Left recuperator, kWt	7,574.8	
Heat delivered to Right recuperator, kWt		4,166.9
Heat acquired in Right recuperator, kWt	3,753.7	
Gross OEC power, kW	20,800	
OEC parasitic power, kW	1,182	
Net OEC power, kW	19,618	

Tables 6 and 7 give the results of calculations for the thermal and exergetic efficiencies. The thermal efficiency, i.e., the ratio of net power output to the total thermal power added to the cycle is a very respectable 15.1%. The utilization efficiency based on the net power relative to the exergy of the incoming geofluid, both steam and brine, is 37.2% while the functional utilization efficiency based on the net power relative to the change in exergy of the geofluid as it passes through the plant is 51.2%. The former efficiency in essence assigns zero exergy to the geofluid as it leaves the plant, whereas the latter takes that exergy into account. Since the exiting geofluid is reinjected and not wasted, the latter may be a more meaningful measure of the utilization of the available geofluid.

Table 6. First Law cycle analysis: thermal efficiency.

Item	Value
Heat into Left preheater from brine, kWt	17,933.8
Heat into Left evaporator from steam, kWt	46,707.1
Heat into Right preheater from condensate, kWt	18,424.0
Heat into Right evaporator from steam, kWt	46,707.1
Total heat rate into cycle, kWt	129,772
Thermal efficiency	0.151

Table 7. Second Law cycle analysis: exergy or utilization efficiency.

Item	Value
Dead-state temperature, oC	25
Dead-state pressure, MPa	0.093
Exergy rate delivered by steam, kW	33,102
Exergy rate delivered by brine, kW	19,588
Total input exergy rate, kW	52,690
Exergy or utilization efficiency	0.372
Exergy rate discharged by steam condensate, kW	144.2
Exergy rate discharged by brine, kW	14,234
Total discharge exergy rate, kW	14,378
Total geofluid exergy change, kW	38,312
Functional exergy efficiency	0.512

Using the definitions and working equations in Ref. [13], the functional utilization efficiencies of the preheater, evaporator, recuperator, and turbine can be determined for the design conditions. The results are given in Tables 8 and 9, for these components on the Left- and Right-sides of the unit, respectively. It will be seen that the corresponding components on each side do not perform identically. The evaporators are the most efficient in terms of collecting exergy from the geofluid, while the recuperators are the worst in terms of the efficiency of exchanging exergy between the low- and high-pressure N-pentane streams. The turbines convert 82-84% of the exergy provided by the N-pentane as it passes through the machines. It must be emphasized that all the results in this section pertain to the design case.

Table 8. Second Law Left-side component analysis: functional utilization efficiency.

Preheater		Evaporator		Recuperator		Turbine	
State	Exergy Rate	State	Exergy Rate	State	Exergy Rate	State	Exergy Rate
	kW		kW		kW		kW
B1	19,588	S2	16,551	2	4,758	1	18,095
B2	14,234	S4	1,791	3	3,423	2	4,758
ΔB	5,354	ΔS	14,761	ΔLP	1,335	Δi-C_5	13,337
8	1,532	9	4,866	6	516	$\dot{W}_T$	11,236
9	4,866	1	18,095	7	1,092		
Δi-C_5	3,335	Δi-C_5	13,229	ΔHP	576		
$\eta_{U\text{-}PH}$	0.623	$\eta_{U\text{-}E}$	0.896	$\eta_{U\text{-}R}$	0.431	$\eta_{U\text{-}T}$	0.843

Table 9. Second Law Right-side component analysis: functional utilization efficiency.

Preheater		Evaporator		Recuperator		Turbine	
State	Exergy Rate	State	Exergy Rate	State	Exergy Rate	State	Exergy Rate
	kW		kW		kW		kW
S6	3,581	S3	16,551	2	3,912	1	15,600
S7	141	S5	1,791	3	3,054	2	3,912
ΔS	3,440	ΔS	14,761	ΔLP	857	Δi-C5	11,689
6	416	7	2,684	7	1,092	$\dot{W}_T$	9,564
7	2,684	1	15,600	8	1,532		
Δi-C_5	2,268	Δi-C_5	12,916	ΔHP	439		
$\eta_{U\text{-}PH}$	0.659	$\eta_{U\text{-}E}$	0.875	$\eta_{U\text{-}R}$	0.513	$\eta_{U\text{-}T}$	0.818

Plant Performance – Acceptance Test Data

The power plant was put to the test on October 3, 2011 to determine its performance relative to the manufacturer's guarantee. The 100% load test was run for a period of four (4) hours from 17:00-21:00 hours during which time 268 readings were recorded. Other tests were conducted for 25, 50, 75 and 110% load conditions [L. Bronicki, Pers. Comm., December 26, 2011]. Only the 100% load results are discussed here.

The following quantities were measured and recorded:

- Dry-bulb temperature
- Relative humidity
- Brine inlet temperature
- Brine inlet pressure
- Brine outlet temperature
- Brine outlet pressure
- Brine mass flow rate
- Steam mass flow rate
- Steam noncondensable gas content
- Gross generator power for OEC 1
- Gross generator power for OEC 2
- Plant net power

Since the performance guarantee is predicated on specific ambient, brine, and steam conditions, a number of correction factors need to be calculated to convert the performance under the conditions actually existing during the test to what the performance would be under the contract specified conditions.

A summary of the 100% load test results are shown in Table 10; all values are averages of 268 raw readings taken at 1 minute intervals over a period of 4 hours. The very small standard deviations indicate that the plant ran at essentially steady-state conditions throughout the test. After all correction factors were applied, the observed average plant net power of 35.36 MW given in the raw data table becomes 37.46 MW. The guaranteed contract value is 35.08 MW, and so the plant met and exceeded the power guarantee.

Two other quantitative items also passed the test: the average brine discharge temperature had to be greater than 140ºC; the corrected test value was 142.1ºC; and the average brine discharge pressure leaving the pumps had to exceed 11.5 bar; the corrected test value was 11.91 bar. Since the acceptance test was focused on only those guaranteed performance parameters, the data recorded was not sufficient to allow a full assessment of the cycle and plant.

Table 10. Performance during acceptance tests on October 3, 2011.

Item	Value	Std. Dev.
Brine mass flow rate, kg/s	461.94	4.68
Brine inlet temperature, °C	165.28	0.20
Brine outlet temperature, °C	142.11	0.16
Steam mass flow rate, kg/s	84.52	0.54
Steam NCG, % (wt. of steam)	0.90	0.00
OEC-1 gross power, MW	20.95	0.08
OEC-2 gross power, MW	20.95	0.04
Plant net power, MW	35.36	0.18

Plant Performance – Availability and Plant Factor

Table 11 presents the operational performance of the plant starting with the first full month of operations through March 2012 (last available data) [Pers. Comm., J.M. Fernández, ICE, April 19, 2012]. The slight downturn in output in December 2011 and January 2012 was mainly caused by a pump failure that necessitated running one unit at a reduced load while the pump was being repaired. Otherwise, the performance has been excellent. Including the forced partial outage, the plant averaged 91.7% availability and 90.1% plant or capacity factor, based on a nominal gross rating of 42 MW over the first eight months of operation.

Table 11. Las Pailas operational data for the first eight months of operation.

Month	Year	Generation	Average Gross Power	Availability Factor	Plant Factor
		MWh	MW	%	%
August	2011	27,113.42	34.99	100.0	86.77
September	2011	29,645.53	41.17	98.47	98.03
October	2011	30,272.86	39.06	99.17	96.88
November	2011	26,644.65	37.01	95.20	88.11
December	2011	23,335.57	30.11	61.59	74.68
January	2012	23,875.87	30.81	79.59	76.41
February	2012	29,117.26	41.84	99.61	99.61
March	2012	31,228.76	40.30	99.78	99.94
Averages		**27,654.24**	**36.91**	**91.68**	**90.05**

Environmental Impact

The environmental management system (EMS) is based on ISO Standard 14001 and includes monitoring all the usual potential environmental impacts plus maintaining good relations with land owners where geothermal activities take place and conformance with the environmental legislation in Costa Rica. ICE also conducts an educational and betterment program for nearby communities.

One part of the EMS is the Environmental Monitoring Program (EMP) in which air quality (H_2S and CO_2 concentrations), rain water (pH), groundwater quality (pH, Cl and conductivity), and noise levels are monitored continuously around the field and neighboring areas. The locations of the measuring stations are shown in Figure 20; there are 15 stations to monitor the groundwater quality and seven more stations to monitor the rain water, air quality and noise levels [14]. These stations were put into operation prior to the startup of plant operations, some going back as far as 2000, to provide a baseline data set against which to measure any impact from plant operations. In addition, as part of a national seismic monitoring effort, the ground levels and seismicity in the RDLV/Las Pailas area are continuously recorded.

In all stations shown in Figure 20, the behavior of the observed variables shows no difference between the current data with the plant running and the long-term baseline data. Thus, so far there is no discernible environmental impact for the measured variables. These variables will continue to be monitored to detect changes that might be attributable to the withdrawal, use, and injection of geofluid. Given the excellent experience with minimal environmental impact at the much larger power plant complex at the neighboring Miravalles field, operating for over 18 years, it is anticipated that similar results will be found at Las Pailas.

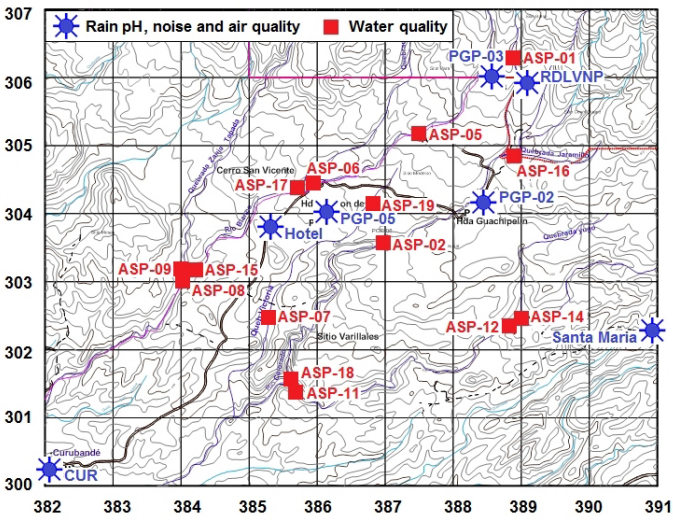

Figure 20. Environmental monitoring stations in the Las Pailas power plant area, after [14].

Conclusions

The Las Pailas geothermal power station is a unique 2-unit binary power plant that uses both the steam and hot brine from a 247ºC (nominal) liquid-dominated reservoir. As of March 2012, 18 wells have been completed, half vertical and half directional, with one well in progress. The plant is served by six production wells while the waste brine is taken by one cold and three hot injection wells. Two essentially identical normal-pentane binary units constitute the plant that is rated at 41.6 MW (gross) and 35 MW (net). Thermodynamically, the plant is designed to produce a thermal efficiency of 15.1%, a utilization efficiency of 37.2% based on the exergy of the incoming geofluid, and a utilization efficiency of 51.2% based on the change in exergy of the geofluid as it passes through the plant. Operating performance for the first eight months of operation has been excellent, with an average capacity factor of 90.1% and an availability factor of 91.7%, including a 2-month period of reduced output caused mainly by a pump failure. So far there are no discernible environmental impacts from plant operations.

Acknowledgements

The authors thank Lucien Bronicki, Ormat, Inc., for providing a summary of the acceptance test, José Manuel Fernández, ICE, for providing the availability and capacity factor data, and Hartman Guido Sequeira, ICE, for providing the environmental monitoring data.

References

[1] "The World Factbook," U.S. Central Intelligence Agency: https://www.cia.gov/library/publications/the-world-factbook/, accessed March 5, 2012.

[2] "Costa Rica Energy Profile," *Renewable Energy Intelligence:* http://www.energici.com/energy-profiles/by-country/central-a-south-america-a-l/costa-rica, accessed March 5, 2012.

[3] Moya, P. and D. Pérez, "Las Pailas Geothermal Project: A 35 MW Plant," *Proc. World Geothermal Congress 2010*, Paper No. 0632, Bali, Indonesia, April 25-29, 2010.

[4] Bodvarsson, G. and D. G. Bailey, "Report of a Mission to Investigate Geothermal Prospects in Costa Rica," Instituto Costarricense de Electricidad, 1963.

[5] "Guanacaste Geothermal Project, Technical Prefeasibility Report", ICE, Rogers Engineering and GeothermEx, Inc., December 1976.

[6] "Estudios de Reconocimiento y Prefactibilidad Geotérmica en la Republica de Costa Rica, Fase I, Estudio de Reconocimiento, Informe Final," ICE, Ente Nazionale per l'Energia Elettrica/ UNG, Pisa, Italy, in collaboration with Electroconsult, Geotermica Italiana and Geosystem, 1989.

[7] Molina, F., "Drilling of gradient wells of the Rincón de la Vieja geothermal field, Departamento de Recursos Geotérmicos, Oficina de Desarrollo Geotérmico, Presentado en la Reunión No 17 del Panel de Consultores de Miravalles, ICE, June 1997.

[8] Moya, P. and A. Yock, "First seven years of exploitation at the Miravalles geothermal field. *Twenty-sixth Workshop on Geothermal Reservoir Engineering*, Stanford University, Stanford, CA, January 29-31, 2001.

[9] Moya, P., F. Nietzen and S. Castro, "Production and Injection at Miravalles and Las Pailas Geothermal Fields," Short Course on Geothermal Development and Geothermal Wells, UNU-GTP and LaGeo, Santa Tecla, El Salvador, March 11-17, 2012.

[10] Moya, P. and R. DiPippo, "Miravalles Unit 3 Single-Flash Plant, Guanacaste, Costa Rica: Technical and Environmental Performance Assessment," *Proc. World Geothermal Congress 2010*, Paper No. 2604, Bali, Indonesia, April 25-29, 2010.

[11] Moya, P. and R. DiPippo, "Miravalles Unit 5 Bottoming Binary Plant: Planning, Design, Performance and Impact," *Geothermics*, V. 36, 2007, pp. 63-96.

[12] National Institute of Standards and Technology (NIST), U.S. Department of Commerce: http://www.nist.gov/srd/nist23.cfm.

[13] DiPippo, R., *Geothermal Power Plants: Principles, Applications, Case Studies, and Environmental Impact, 3rd. Ed.*, Butterworth-Heinemann: Elsevier, Oxford, England, 2012.

[14] Guido, H., "Informe Gestión Ambiental Las Pailas," *ICE Internal Report*, Primer Trimestre, 2012, Bagaces, Guanacaste, March 2012 [In Spanish].